

## Formation of nano- and microstructured layers of silver during thermal destruction of polyvinyl alcohol with silver nitrate

© A.I. Sidorov,<sup>1,2</sup> P.A. Bezrukov,<sup>1</sup> A.V. Nashchekin,<sup>3</sup> N.V. Nikonorov<sup>1</sup>

<sup>1</sup> ITMO University,  
199034 St. Petersburg, Russia

<sup>2</sup> St. Petersburg State Electrotechnical University „LETI“,  
197376 St. Petersburg, Russia

<sup>3</sup> Ioffe Institute,  
194021 St. Petersburg, Russia  
e-mail: sidorov@oi.ifmo.ru

Received April 9, 2022

Revised May 19, 2022

Accepted May 21, 2022

The results of experimental study of morphology of silver nanostructures, which appear during thermal destruction of polyvinyl alcohol film with silver nitrate are presented. It is shown that during the increase of silver nitrate concentration the maximum size of the formed particles increases from tens of nanometers up to 2  $\mu\text{m}$ , and their shape transforms from spherical to irregular. The growth of silver nanoparticles occurs at the expense of small silver nanoparticles migration on a substrate surface, their gathering near the large nanoparticles and confluence of small nanoparticles with larger ones.

**Keywords:** nanoparticle, silver, polyvinyl alcohol, morphology, absorption, luminescence .

DOI: 10.21883/TP.2022.09.54682.91-22

### Introduction

Metal nanoparticles are widely used in photonics and plasmonics, in telecommunications and information processing devices, for the detection of chemicals and in medicine, as well as in plasmonic devices based on the amplification of luminescence and Raman scattering under conditions of local amplification of the electromagnetic wave field amplitude at plasmon resonance [1–4]. Nanoparticles and nanoporous layers of silver and gold are used in the photocatalytic decomposition of water [5–7]. For metal nanoparticles synthesis the chemical reactions in liquid and polymer media [8–10], electrochemical methods [11], vacuum deposition or laser ablation on a substrate [12,13], ion implantation [14,15] and a number of other methods can be used. The paper [16] describes the possibility of obtaining nanostructures based on silver by thermal decomposition of silver nitrate dissolved in polyvinyl alcohol (PVA).

The mechanisms of formation and growth of a fractal ensemble of nanoparticles essentially depend on the method and conditions of its synthesis. As a rule, to describe these processes the aggregation models of nanoparticle–cluster [17–20] are used. The most common association models used are diffusion-limited aggregation and ballistic aggregation.

For sensor applications, not only small (less than 100 nm) isolated metal nanoparticles with plasmon resonance are

of interest, but also ensembles of metal nanoparticles that form fractal clusters in which electromagnetic interaction between nanoparticles occurs. In such clusters, as a result of the interaction of surface plasmons, „hot spots“ occur, in which the local amplification of the electromagnetic wave field amplitude can exceed  $10^4$  [21,22]. This leads to the amplitude of the Raman scattering increasing and, accordingly, to the sensitivity increasing of chemical and biosensors.

The aim of this paper was to analyze the optical properties and morphology of nanostructured silver layers obtained by thermal decomposition of PVA film with silver nitrate, as well as to study the processes that affect the morphology of the formed nanostructured layers.

### 1. Experimental procedure

Nanostructured silver layers were fabricated using aqueous solutions of  $\text{AgNO}_3$  with concentrations of 0.25, 0.5, 1, and 2 wt.%. Solutions of  $\text{AgNO}_3$  were mixed with an aqueous solution of PVA (concentration 0.03 wt.%). PVA with a relative molecular weight of 25 000 was used.

Polished soda silicate glass plates were used as substrates. After applying a thin layer of the solution to the substrate, the samples were dried in the dark for 24 h.

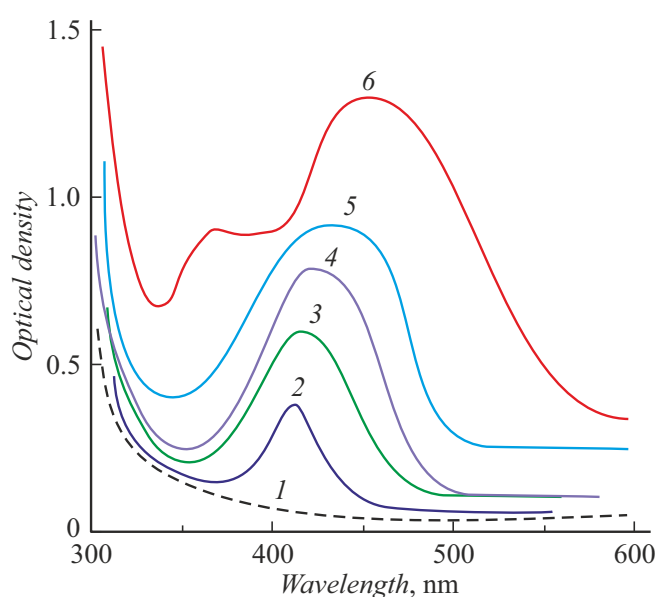
Heat treatment of the samples was carried out in muffle furnaces (Nabertherm) in air atmosphere at a temperature of  $T = 300^\circ\text{C}$  for 10 min. The optical density spectra of the samples were measured using Lambda 500 spectrophotometer (Perkin Elmer). Luminescence spectra were measured using a LS55 spectrofluorimeter (Perkin-Elmer). Optical measurements were performed at room temperature. The morphology of the nanostructured silver layer after heat treatment was studied using a scanning electron microscope (SEM) JSM 7001F (JEOL).

## 2. Results and discussion

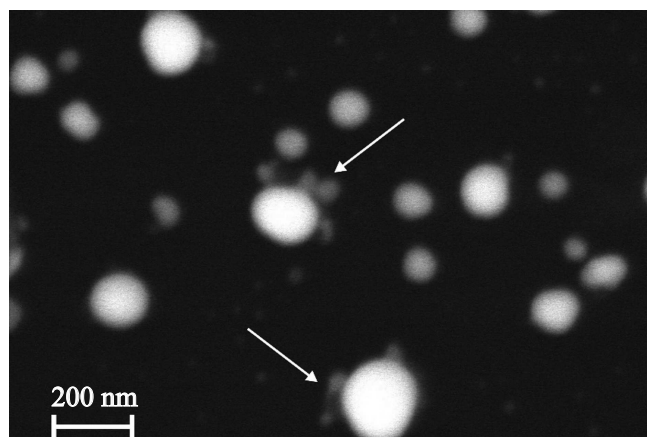
Initially, before drying, the mixture of  $\text{AgNO}_3$  and PVA solutions is colorless. After drying in the dark the PVA film becomes light yellow at a low concentration of  $\text{AgNO}_3$  and yellow-brown at a high concentration of  $\text{AgNO}_3$ . At that, an absorption band appears on the optical density spectrum near the wavelength  $\lambda = 410$  nm (Fig. 1, curve 2). This band corresponds to the plasmon resonance of spherical silver nanoparticles smaller than 20 nm [1,4]. Thus, already at the stage of drying silver nanoparticles are formed in PVA. Heat treatment at  $T = 300^\circ\text{C}$  leads to the amplitude increasing of the plasmon absorption band and its broadening (Fig. 1, curve 3). The  $\text{AgNO}_3$  concentration increasing is accompanied by the amplitude increasing of the plasmonic absorption band, its broadening, and a long-wavelength spectral shift (Fig. 1, curve 4). At the maximum concentration of  $\text{AgNO}_3$  an additional absorption maximum appears at  $\lambda = 370$  nm (Fig. 1, curve 5). The broadening of the plasmonic absorption band, its long-wavelength spectral shift and the appearance of an additional absorption maximum are associated with the size increasing of nanoparticles and with the electromagnetic interaction of closely spaced nanoparticles [1,4].

Fig. 2 shows the SEM image of silver nanoparticles after heat treatment for an  $\text{AgNO}_3$  concentration of 0.25 wt.%. It can be seen from the Figure that during heat treatment silver nanoparticles are formed on the substrate, which have a shape close to spherical. The largest nanoparticles have sizes of 150–200 nm. Most of the nanoparticles have an average size of less than 50 nm. Smaller sizes of nanoparticles correspond to their higher concentration on the substrate surface. It can be seen from Fig. 2 that small nanoparticles are grouped near larger nanoparticles (marked with arrows in Fig. 2).

Fig. 3 shows the SEM image of silver nanoparticles after heat treatment for an  $\text{AgNO}_3$  concentration of 0.5 wt.%. The  $\text{AgNO}_3$  concentration increasing leads to the maximum size of nanoparticles increasing up to 250 nm. In this case, the shape of the largest nanoparticles differs from spherical. The concentration of silver nanoparticles on



**Figure 1.** Optical density spectra of samples: 1 — substrate before application of PVA layer; 2 — after drying the PVA layer with  $\text{AgNO}_3$  ( $\text{AgNO}_3$  concentration 0.25 wt.%); after heat treatment at temperature  $T = 300^\circ\text{C}$  and  $\text{AgNO}_3$  concentration (in wt.%): 3 — 0.25, 4 — 0.5, 5 — 1, 6 — 2.



**Figure 2.** SEM image of silver nanoparticles after heat treatment.  $\text{AgNO}_3$  concentration 0.25 wt.%. Arrows indicate grouping of small silver nanoparticles near larger nanoparticles.

the substrate increases compared to the case described above.

With further  $\text{AgNO}_3$  concentration increasing to 1 wt.%, microparticles of irregular shape appear, with sizes exceeding  $1\ \mu\text{m}$  (Fig. 4). The concentration of such microparticles is low. At the same time a large number of nanoparticles is formed with sizes of 200–250 nm and below 100 nm.

At  $\text{AgNO}_3$  concentration of 2 wt.% heat treatment leads to a large number of irregularly shaped silver microparticles

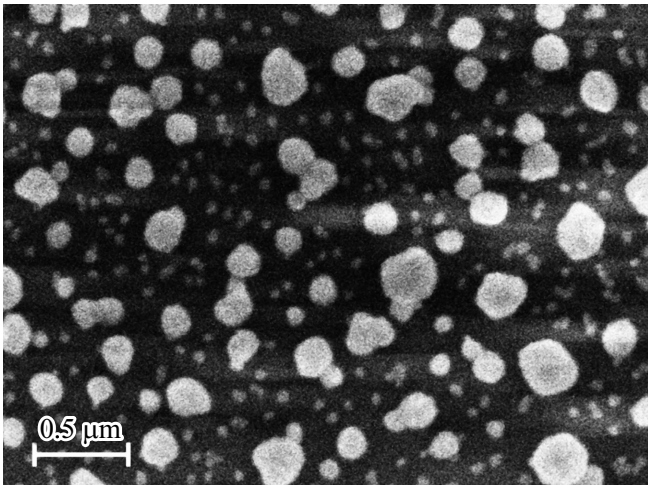


**Figure 3.** SEM image of silver nanoparticles after heat treatment.  $\text{AgNO}_3$  concentration is 0.5 wt.%.

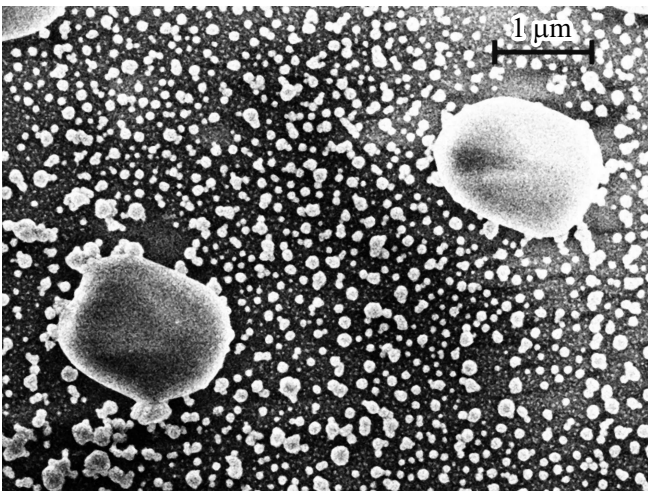


**Figure 4.** SEM image of silver nano- and microparticles after heat treatment.  $\text{AgNO}_3$  concentration 1 wt.%.

with the size of  $0.5\text{--}2\ \mu\text{m}$  appearance on the glass surface (Fig. 5). At the same time, there are also silver nanoparticles with the size of  $100\text{--}250\ \text{nm}$ , which have a shape close to spherical.

After the silver nano- and microstructures removal from the glass surface by etching in nitric acid a broadband luminescence in the visible region of the spectrum was detected in a thin near-surface layer of the glass. The luminescence spectra are shown in Fig. 6. Such luminescence is characteristic for  $\text{Ag}^+$  ions,  $\text{Ag}^0$  neutral atoms, and subnanosize molecular clusters of silver  $\text{Ag}_n$  ( $n = 2\text{--}4$ ) [23,24]. The contribution to the luminescence in the spectral range  $450\text{--}470\ \text{nm}$  can be associated with ions, neutral atoms, and  $\text{Ag}_4$  silver molecular clusters. Luminescence near the wavelength  $500\ \text{nm}$  is typical for neutral molecular clusters of silver  $\text{Ag}_2$ . Lumines-

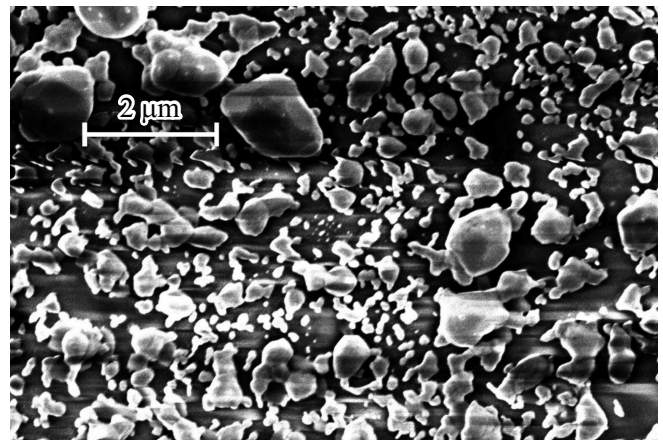


**Figure 5.** SEM image of silver nano- and microparticles after heat treatment.  $\text{AgNO}_3$  concentration is 2 wt.%.

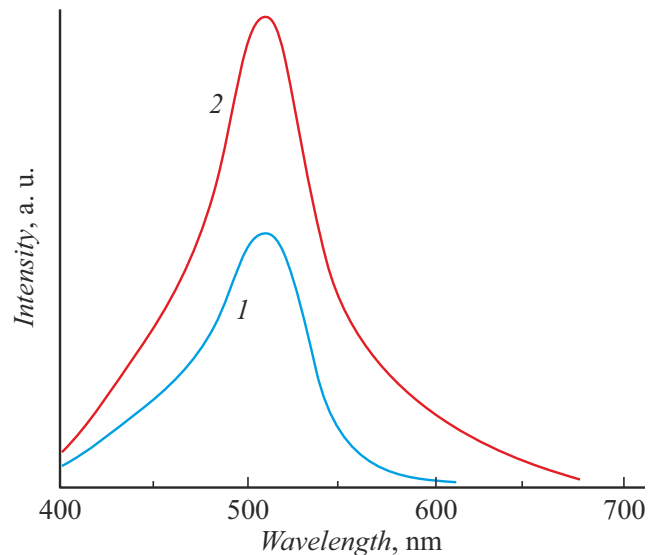
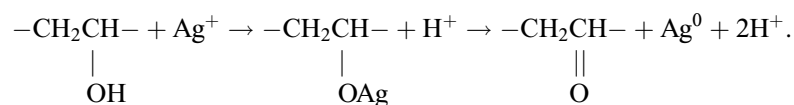


**Figure 6.** Luminescence spectra of samples after removal of nano- and microparticles of silver from the surface: 1 —  $\text{AgNO}_3$  concentration is 1 wt.%. 2 —  $\text{AgNO}_3$  concentration is 2 wt.%. Luminescence excitation wavelength is  $330\ \text{nm}$ .

cence in the spectral range  $600\text{--}650\ \text{nm}$  indicates the presence of neutral molecular clusters of  $\text{Ag}_3$  in the glass.

As shown above, the formation of silver nanoparticles occurs already at the stage of drying the PVA solution with  $\text{AgNO}_3$  (Fig. 1, curve 2). The reason for this is the following. When silver nitrate solution is mixed with PVA solution, chemical bonds with hydrogen in the hydroxyl groups in the PVA molecular chains are broken. As a result, free bonds of PVA hydroxyl groups are bound to  $d$ - and  $f$ -orbitals of  $\text{Ag}^+$  ions. After that, the separation of neutral silver atoms from the hydroxyl groups and the formation of nanoparticles from them are possible.

These processes can be written as follows [25]:



At the stage of melting and thermal decomposition of the PVA film ( $T = 220\text{--}230^\circ\text{C}$ ), small silver nanoparticles migrate over the substrate surface and group near larger nanoparticles (Fig. 3). After that, the integration of small silver nanoparticles with larger nanoparticles is possible. This process is similar to the processes described in the Ostwald theory of ripening [26,27].

Note that the processes described above occur at temperatures much lower than the melting point of silver ( $T_m = 980^\circ\text{C}$ ). At the same time, it is known that as the nanoparticle size decreases, its melting point decreases too [28,29]. The reason for this is the quantum-confined effects leading to a change in the phonon spectrum. However, a noticeable decreasing of the melting temperature takes place at nanoparticle sizes below 10 nm. Therefore, we can conclude that the processes associated with melting do not participate in the observed effects.

Despite the fact that silver ions have a luminescence band in the spectral range of 450–470 nm, in our case, luminescence cannot be associated with them. Silver ions cannot penetrate the glass when it is heated, as this violates the electrical neutrality of the glass. The introduction of  $\text{Ag}^+$  from the silver layer into sodium-silicate glass is possible only with solid-state ion exchange in the presence of the electric field [30]. Neutral silver atoms can penetrate into the surface layers of glass as a result of thermal diffusion. In silicate glasses silver atoms are grouped near glass network defects [31]. At their sufficient concentration some of them form luminescent subnanosized molecular clusters. Similar effects were observed during thermal dissolution of continuous films of silver and gold in silicate glass [32].

## Conclusion

Thus, the thermal decomposition of PVA film with silver nitrate results in the formation of silver nano- and microparticles. With the concentration of silver nitrate increasing, the maximum size of the formed nano- and microparticles increases from tens of nanometers up to  $2\ \mu\text{m}$ , and their shape becomes irregular. The growth of silver nanoparticles occurs due to the migration of small silver nanoparticles over the substrate surface, grouping them near larger nanoparticles and further integration of small silver nanoparticles with larger nanoparticles is possible. Some of the silver atoms penetrate into the near-surface layer of the glass substrate and form luminescent subnanosized molecular clusters.

## Acknowledgments

The electron microscopic studies were performed using the equipment of the Federal Common Use Centre „Materials Science and Diagnostics in Advanced Technologies“, supported by the Ministry of Education and Science of Russia.

## Funding

This study was financially supported by the Russian Science Foundation (project № 20-19-00559).

## Conflict of interest

The authors declare that they have no conflict of interest.

## References

- [1] V.V. Klimov. *Nanoplasmonics* (Pan Stanford, Singapore, 2014), DOI: 10.1201/b15442
- [2] M. Eichelbaum, K. Rademann. *Adv. Funct. Mater.*, **19**, 2045 (2009). DOI: 10.1002/adfm.200801892
- [3] Y. Chen, L. Karvonen, A. Säynätjoki, C. Ye, A. Tervonen, S. Honkanen. *Opt. Mater. Expr.*, **1**, 164 (2011). DOI: 10.1364/OME.1.000164
- [4] *Silver Nanoparticles*, ed. D.P. Perez (In-Tech, Vukovar, Croatia, 2010), DOI: 10.1007/978-1-4020-9491-0\_22
- [5] S. Linic, P. Christopher, D.B. Ingram. *Nature Mater.*, **10**, 911 (2011). DOI: 10.1364/OE.25.012753
- [6] M. Graf, D. J alas, J. Weissmüller, A.Y. Petrov, M. Eich. *ACS Catal.*, **9**, 3366 (2019). DOI: 10.1021/ACSCATAL.9B00384
- [7] A.N. Koya, X. Zhu, N. Ohannesian, A.A. Yanik, A. Alabastri, R.P. Zaccaria, R. Krahne, W.-C. Shih, D. Garoli. *ACS Nano*, **15**, 6038 (2021). DOI: 10.1021/acsnano.0c10945
- [8] L.A. Dykman, V.A. Bogatyrev, S.Yu. Schegolev, N.G. Khlebtsov. *Zolotyie nanochastitsy: sintez, svoystva, biomeditsinskoe primeneniye* (Nauka, M., 2008) (in Russian)
- [9] S.V. Karpov, V.V. Slabko. *Opticheskie i fotofizicheskie svoystva fraktal'no-strukturirovannykh zoley metallov* (Izdvo SO RAN, Novosibirsk, 2003) (in Russian)
- [10] L. Shang, S. Dong, G.U. Nienhaus. *Nano Today*, **6**, 401 (2011). DOI: 10.1016/J.NANTOD.2011.06.004
- [11] B.S. Gonzalez, M.J. Rodriguez, C. Blanco, J. Rivas, M.A. Lopez-Quintela, J.M.G. Martinho. *Nano Lett.*, **10**, 4217 (2010). DOI: 10.1007/978-94-007-6178-0\_55-2
- [12] A.P. Boltaev, N.A. Penin, A.O. Pogosov, F.A. Pudonin. *ZhETF* **123**, 1067 (2003) (in Russian)
- [13] V.I. Egorov, I.V. Zvyagin, D.A. Klyukin, A.I. Sidorov. *J. Opt. Technol.*, **81** (5), 270 (2014). DOI: 10.1364/JOT.81.000270
- [14] R.A. Ganeev, A.I. Rysanyanskii, A.L. Stepanov, M.K. Kondirov T. Usmanov. *Opt. Spectr.*, **95**, 967 (2003). DOI: 10.1134/1.1635484

- [15] A.L. Stepanov. *Rev. Adv. Mater. Sci.*, **4**, 45 (2003).
- [16] Q. Zhang, X. Wang, J. Jiang, H. Yao, Q. Nie, Z. Bai. *Opt. Mater. Expr.*, **11**, 1504 (2021). DOI: 10.1364/OME.424275
- [17] V.M. Samsonov, Yu.V. Kuznetsova, E.V. D'yakova. *Tech. Phys.*, **61**(2), 227 (2016).  
DOI: 10.1134/S1063784216020201
- [18] B.M. Smirnov. *UFN*, **149**(2), 177 (1986) (in Russian)
- [19] R. Jullien. *Comm. Cond. Mat. Phys. (Comm. Mod. Phys. Pt. B)*, **13**, 4, 177 (1987).
- [20] T.A. Witten, L.M. Sander. *Phys. Rev. B*, **27**, 5686 (1983).
- [21] *Surface-Enhanced Raman Scattering*, ed. K. Kneipp, H. Moskovits (Springer, NY., 2006)
- [22] D.V. Yakimchuk, E.Y. Kaniukov, S. Lepeshov, V.D. Bundyukova, S.E. Demyanov, G.M. Arzumanyan, N.V. Doroshkevich, K.Z. Mamatkulov, A. Bochmann, M. Presselt, O. Stranik, S.A. Khubezhov, A.E. Krasnok, A. Alú, V.A. Sivakov. *J. Appl. Phys.*, **126**, 233105 (2019).  
DOI: 10.1063/1.5129207
- [23] S. Fedrigo, W. Harbich, J. Buttet. *J. Chem. Phys.*, **99**, 5712 (1993). DOI: 10.1063/1.465920
- [24] V.D. Dubrovin, A.I. Ignatiev, N.V. Nikonorov, A.I. Sidorov, T.A. Shakhverdov, D.S. Agafonova. *Opt. Mater.*, **36**, 753 (2014). DOI: 10.1016/j.optmat.2013.11.018
- [25] K.L. Liang, Y.C. Wang, W.L. Lin, J.J. Lin. *RSC Adv.*, **4**, 15098 (2014). DOI: 10.1039/C4RA00402G
- [26] W. Ostwald. *Z. Phys. Chem.*, **34**, 495 (1900).
- [27] C. Wagner. *Z. Electrochem.*, **63**, 581 (1961).
- [28] N.S. Sdobnyakov, V.M. Samsonov, A.N. Bazulev, D.A. Kyul'pin. *Bull. Russ. Acad. Sci. Phys.*, **72**, 1371 (2008). DOI: 10.1134/S1027451018050671
- [29] V.M. Samsonov, N.Yu. Sdobnyakov, V.S. Myasnichenko, I.V. Talyzin, V.V. Kulagin, S.A. Vasilyev, A.G. Bembel, A.Yu. Kartoshkin, D.N. Sokolov. *J. Surf. Investig.*, **12**, 1206 (2018). DOI: 10.1134/S1027451018050671
- [30] A. Tervonen, S. Honkanen, M. Leppihalme. *J. Appl. Phys.*, **62**, 759 (1987).
- [31] *Defects in SiO<sub>2</sub> and Related Dielectrics: Science and Technology*. NATO Science Series II. V. 2, ed. by G. Pacchioni, L. Skuja, D.L. Griscom (Dordrecht, Kluwer, 2000)
- [32] A.V. Nashchekin, M.V. Pogumirskii, P.V. Rostokin, A.I. Sidorov, T.A. Shakhverdov. *Phys. Solid State*, **57**, 1659 (2015). DOI: 10.1134/S1063783415080211